

# MODEL FOR PREDICTING THE RESULTS OF TENSILE TEST WITH STRAIN RATE DEPENDENT PLASTICITY AND THE STRAIN DISTRIBUTION AT THE END OF THE STRAIN PROCESS

JOZEF KMEC<sup>1</sup>, JOZEF PAVELKA<sup>1</sup>, JAROSLAV SOLTES<sup>1</sup>

<sup>1</sup>Faculty of Humanities and Natural Sciences, Presov University, Presov, Slovakia

DOI: 10.17973/MMSJ.2023\_10\_2023007

e-mail to corresponding author: jozef.kmec@unipo.sk

In this article, the attention was focused on the possibilities of determining material properties (at the reference strain rate), which are obtained from the experiment using a suitable material model, Curve fitting toolbox, custom-made software (Matlab computing core), which are necessary for the results prediction of the tensile test with plasticity depending on the rate of deformation or for the strain distribution at the end of the strain process in material samples.

## KEYWORDS

Matlab, original Johnson-Cook model, material parameters, strain distribution.

## 1 INTRODUCTION

For the results prediction of a tensile test with plasticity dependent on the rate of deformation (or pressability of steel sheets) by numerical simulation, in addition to the tool model, pressing kinematics, the following material data are required:  $\nu$  - Poisson's number,  $E$  - modulus of elasticity, curves of natural deformation resistances in the form of suitable material models: Johnson-Cook model (applied in this article), Hollomon model, Krupkowsky model, etc., course of the strengthening curve point by point from the recording of the tensile test,  $r$  - coefficient of normal anisotropy (for steel sheets in the direction of  $0^\circ$ ,  $45^\circ$ ,  $90^\circ$ ), FLC - Forming limit curves, the value of maximum thinning or deformation in the direction of the thickness of the sheet,  $f$  - coefficient of friction [Vlk 2003].

Suppliers of software for pressing processes simulation as well as sheet metal processors using software simulation products consider the database material their intellectual property due to the time and financial complexity of their detection; and therefore, such data are not public available or freely distributed in most cases [Huang 2002, Murcinkova 2013, Bozek 2021].

In case of more complex shapes of extrusions from new types of sheets, it is difficult to predict the pressability (manufacturability) of steel sheets based on the values of mechanical properties, because pressability depends not only on the values of mechanical properties, but also on the state of tension, the rate of deformation, the geometry of the tool and the pressing- conditions [Hlavac 2018, Krenicky 2022].

Powerful computer technology and program files based on the finite element method make it possible to simulate the influence of individual factors on the pressability and quality of the stampings. The maximum approximation of the simulation results to the results of practical pressing depends on:

used simulation software, used material model, completeness of material data, determination of limiting conditions (relative thinning of the wall, pressure and friction on contact surfaces and etc.).

## 2 EXPERIMENT DESCRIPTION

For the purposes of numerical simulation, DC 04 steel sheets were used - particularly deep-drawn, suitable for demanding external and internal parts of car bodies and other extrusions (determination of material parameters at a reference strain rate of  $0.0014s^{-1}$ , which corresponds to the speed of movement of the crossbar of the testing machine  $v_2 = 10$  mm/ min. Samples for testing mechanical properties were taken in the direction of  $90^\circ$  to the direction of rolling and produced according to STN ISO 10002:2021-06 (01 0310), see Fig. 1. Five samples were used to determine one average value of the mechanical property. Tensile tests to determine the material parameters were carried out on the INSTRON tensile testing machine in the U.S. Steel, with hand limited at the selected reference strain rate of  $0.0014s^{-1}$  [Evin 2016].

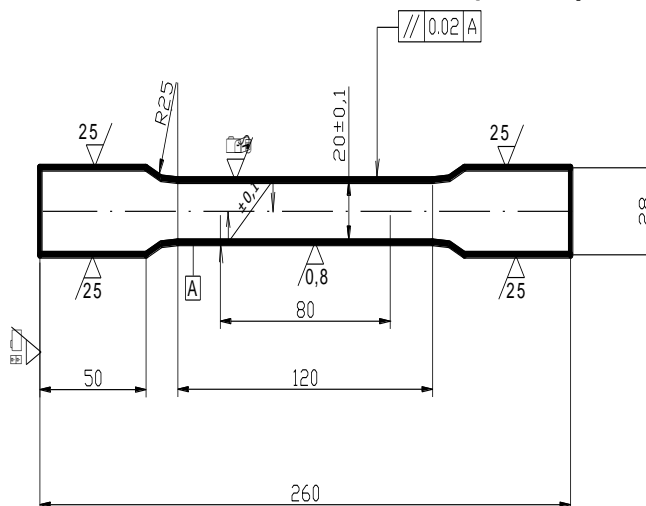


Figure 1. Shape and dimensions of the sample

## 3 PROGRAM OPTIONS MATLAB AND COMSOL MULTIPHYSICS

Matlab is an integrated environment for scientific and technical calculations, modeling, simulation, presentation and data analysis. It is a tool both for comfortable interactive work and for the development of a wide range of applications. Matlab provides powerful graphics, calculation tools and extensive libraries of functions. The extremely fast computing core with optimal algorithms is considered to be Matlab's strongest point. The open architecture led to the creation of libraries of functions, which are called toolboxes, and which expand the use of the program in relevant scientific and technical fields. These designed libraries offer pre-processed specialized functions that can be extended and modified. Matlab allows you to import standard data files

into your environment, to which the Curve Fitting toolbox is applied for their quick processing - use of standard or custom models. Comparison of results is possible either visually or through statistics [Mathworks R2014a].

Comsol Multiphysics is a tool designed for modeling and simulating several physics phenomena. Most of the tasks we encounter in real life have a multiphysics character. Therefore, when developing products or processes and studying the behavior of systems, it is often necessary to consider the mutual interaction of several physical factors at the same time. This means, that Comsol Multiphysics was developed to solve mainly complex physics problems. It consists of a core and a whole range of add-on modules that expand the possibilities of specialized tasks in the field of elasticity of strength (Mechanical), fluid mechanics (Fluids) and many others. The advantage of COMSOL Multiphysics is the direct connection with CAD tools or MATLAB software [COMSOL Multiphysics 2020, COMSOL 2023].

#### 4 RESULTS AND DISCUSSION

When a metal is deformed plastically at a high strain rate, the hardening function will exhibit higher values than at quasistatic conditions. The Johnson-Cook material model is used to simulate this behavior for a tensile test run at different loading rates (For the purpose of numerical simulation, in this article, a reference quasi-static strain rate is of  $0.0014s^{-1}$ ). The stress-strain data obtained from uniaxial tensile tests under different strain rates can be used to determine the material constants of the constitutive equation. The original Johnson-Cook model can be expressed as:

$$\sigma = (A + B\varphi^n)(1 + C \ln \dot{\varphi}^*)(1 + mT^*), \quad (1)$$

where  $\sigma$  is the true stress,  $\varphi$  is the true plastic strain,  $A$  is the initial yield stress at a reference strain rate,  $B$  is the coefficient of strain hardening,  $n$  is the strain hardening exponent,  $C$  and  $m$  are material constants which represent the strain rate coefficient and thermal softening exponent, respectively,  $\dot{\varphi}^* = \dot{\varphi}/\dot{\varphi}_0$  is the dimensionless strain rate ( $\dot{\varphi}$  is the strain rate, while  $\dot{\varphi}_0$  is the reference strain rate), and  $T^*$  is the homologous temperature and expressed as  $T^* = (T - T_r)/(T_m - T_r)$ .

Here,  $T$  is the absolute temperature,  $T_m$  is the melting temperature and  $T_r$  is the reference temperature. It can be found that the original Johnson-Cook model requires fewer material constants and also fewer experiments to evaluate these constants. Johnson-Cook model assumes that thermal softening, strain rate hardening and strain hardening are three independent phenomena and can be isolated from each other. Actually, the coupled effects of temperatures, strain rates and strain on the flow behaviors of the alloy steel should be considered. The reference strain rate is the one at which parameters are determined for the original Johnson-Cook model [Wang 2021, Lin 2010, Johnson 1983, Kuncicka 2021].

In this case, the measurement on the Instron drawing machine was carried out at a constant room temperature, so that the term for thermal softening is unitary and thus there was a need to determine four parameters  $A$ ,  $B$ ,  $C$ , and  $n$  at the reference deformation rate, which are listed in Table 1. The

material constants of the Johnson-Cook constitutive equation were established here simultaneously by fitting the strengthening curves (Curve fitting toolbox - General model). Parameters  $n$ , and  $B$  were determined by non-linear methods of least squares obtained by standardized tensile tests in combination with the methodology for determining the index sensitivity to strain rate (the strain rate coefficient)  $C$ , see equation (2) and with the creation of a custom program in Matlab for determining the  $A$  parameter [Evin 2001].

General model:

$$f(x) = (A+B \cdot x^n) \cdot (1+C \cdot \log(2))$$

Coefficients (with 95% confidence bounds):

$A=144$  (fixed at the bound) - determined from our own tailor-made program

$B = 419$  (fixed at the bound) - determined by fitting

$C = 0.016$  (fixed at the bound) - calculated from equation (2)

$n = 0.5823$  (0.5816, 0.583) - determined by fitting

Goodness of fit: R-square: 0.9795

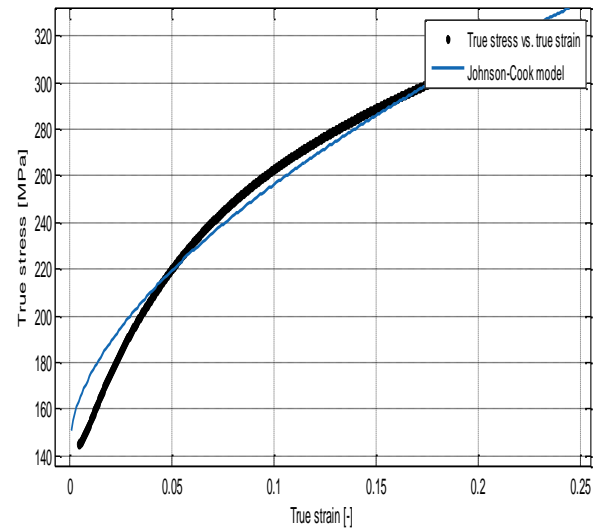


**Figure 2.** Dependence of the True stress versus True strain in the plastic region for the Johnson-Cook model and for the measured experiment carried out on the INSTRON.

In general, it can be stated that as the rate of deformation increases, the metal's resistance to plastic deformation increases as well.

If we proceed from the assumption that the following is valid:  $\dot{\varphi}_1/\dot{\varphi}_{0ref} = v_1/v_{0ref}$  and  $\sigma_1/\sigma_0 = F_1/F_0$ , then the strain rate coefficient can be expressed in the form:

$$C = \frac{\ln(\sigma_1/\sigma_0)}{\ln(\dot{\varphi}_1/\dot{\varphi}_{0ref})} = \frac{\ln(F_1/F_0)}{\ln(v_1/v_{0ref})}, \quad (2)$$

where  $\dot{\varphi}_{0ref}$  is reference strain rate at quasi-static strain rate,  $v_{0ref}$  is reference speed of crossbar of the tensile testing machine.

Before starting the simulation itself, a suitable

- sample geometry must be selected (the sample dimensions are the same as used in the tensile testing machine - Instron).

A 260 mm long test specimen having 20 mm in its central section is used. Its geometry is shown in Figure 1, 3.

Axisymmetry is assumed, and only one quarter of the specimen is modeled due to the symmetry in the axial directions. In Figure 3, a general overview of the stress state is shown for the highest loading rate. The stress in the central

part is about 294 MPa, whereas the initial yield stress is 145 MPa.

- choose of User-controlled mesh.
- boundary conditions

At the thick end of the specimen, the displacement is prescribed in the axial direction. The displacement varies linearly with time, and the maximum elongation of the specimen is of 13 mm. This elongation corresponds to the average strain of 8-10%, but since the plastic deformation occurs only in the thinner part of the specimen, the true plastic strains will be of the order 10 - 20%.

- The material is deep-drawn steel sheets DC 04 with properties as shown in Table 1

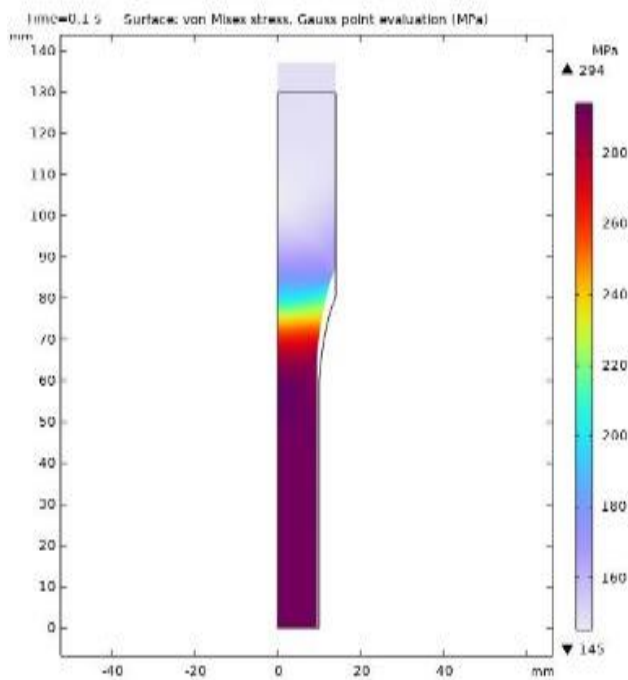


Figure 3. Geometry of the test specimen and von Mises stress on the surface at the end of the tensile test at the strain rate 1/s for a time of 0.1 s.

Table 1. Material properties

PROPERTY	SYMBOL	VALUE
Young's Modulus	$E$	210 GPa
Poisson's ratio	$\nu$	0.29
Initial yield strength	$\sigma_{ys0}$	144 MPa
Strength coefficient	$k$	419 MPa
Hardening exponent	$n$	0.5
Reference strain rate	$\dot{\phi}_0$	0.0014 1/s
Strain rate strength coefficient	$C$	0.016
Reference temperature	$T_{ref}$	293.15 K
Mass density	$\rho$	7850 kg/m <sup>3</sup>

The material constants are calculated at a crossbar movement speed of 10mm/min. The Trust-Region algorithm was used in this calculation. The influence of the strain rate is shown in Figure 4. The axial true stress at the center of the sample is plotted as a function of the axial true strain. Since the stress state is close to uniaxial, this graph essentially shows the constitutive law. For the four lower strain rates, the strain rate hardening effect is negligible. It becomes more significant when the strain rate approaches 1s<sup>-1</sup>. It can be assumed that for quasi-static relative strain rates (up to

$\dot{\epsilon} = 1.s^{-1}$ ), the influence of the relative strain rate will not be more pronounced, the changes will basically move within the marked tendencies.

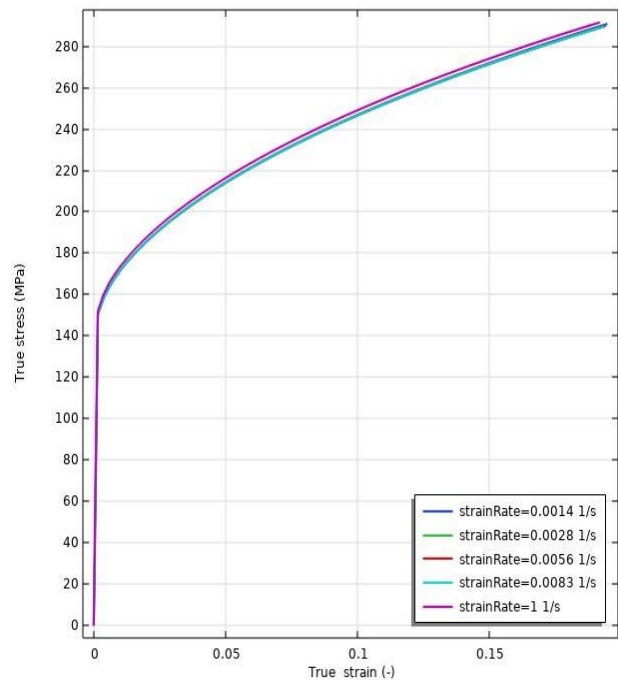


Figure 4. Axial true stress and true strain at the center of the test specimen for the five tensile tests at different strain rates.

In Figure 5 the plastic strain distribution at the end of the strain process is shown for the lowest reference strain rate. At the lower strain rates, the maximum plastic deformation occurs in the central parts of the sample and has a value of max=0.193, whereas at the higher strain rate 1 s<sup>-1</sup>, the peak value actually occurs in a region closer to the loaded end and has a value of max=0.186, see Figure 6.

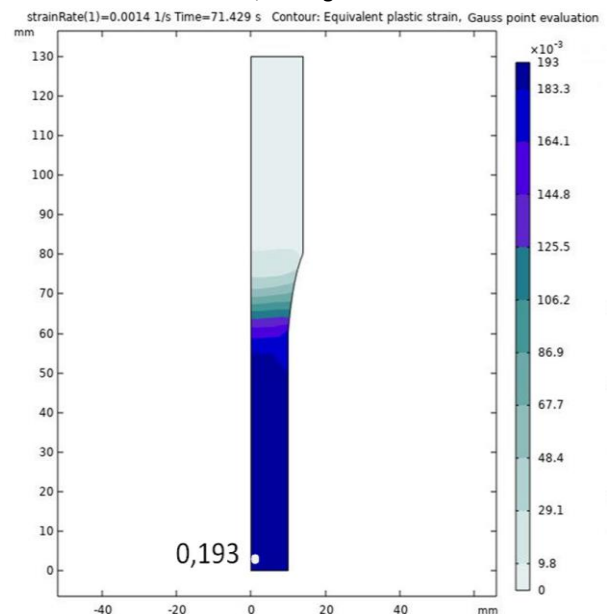
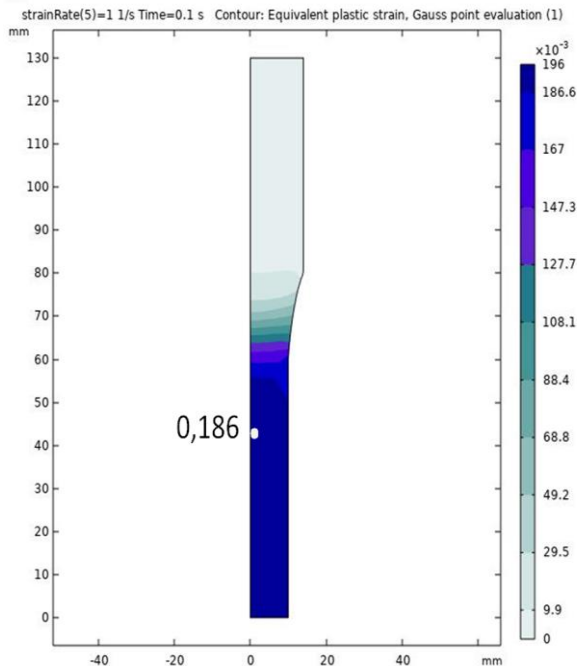


Figure 5. Distribution of plastic strain at the end of the deformation process for the lowest reference strain rate of 0.0014 s<sup>-1</sup>.

At the lowest strain rate of 0.0014 s<sup>-1</sup>, the whole process takes 71.4 seconds. There is thus enough time for a substantial redistribution of the temperature field. At the highest loading rate of 1s<sup>-1</sup>, the whole process takes only 0.1s.

Temperature field to a large extent matches the strain distribution, since the time is not sufficient for any substantial diffusion of heat. Different lengths of strain processes at different strain rates can be conveniently used in the industrial pressing of stampings [Labellarte 2000].



**Figure 6.** Distribution of plastic strain at the end of the deformation process for the highest strain rate of  $1 \text{ s}^{-1}$ .

All analyses were performed using an assumption of geometric linearity in order to speed up analysis and simplify comparisons. However, in reality, geometric nonlinearity should be taken into account.

## 5 CONCLUSION

From the model of predicting the results of the tensile test with plasticity dependent on the rate of strain by numerical simulation it follows that:

- The plastic strain distribution at the end of the strain process at the lowest strain rate occurs in the central part of the sample and has a maximum value of  $\max=0.193$ , while when increasing the strain rate up to a value of  $1 \text{ s}^{-1}$ , the peak value of deformation actually occurs in a region closer to the loaded end and has a value of  $\max=0.186$ .
- At the lowest loading rate of  $0.0014 \text{ s}^{-1}$ , the whole strain process takes 71.4 s, while at the highest loading rate of  $1 \text{ s}^{-1}$ , the whole process takes only 0.1 s. In the automotive industry, under pressure to reduce the production time of stampings by surface forming operations, this fact cannot be ignored.
- For the four lower strain rates ( $0.0014 \text{ s}^{-1}$ ,  $0.0028 \text{ s}^{-1}$ ,  $0.0056 \text{ s}^{-1}$ ,  $0.0083 \text{ s}^{-1}$ ), the effect of strengthening by deformation rate is not significant. It becomes more significant when the strain rate approaches  $1 \text{ s}^{-1}$ .

## REFERENCES

[Bozek 2021] Bozek, P., Nikitin, Y., Krenicky, T. The Basics Characteristics of Elements Reliability. In: Diagnostics of Mechatronic Systems. Series:

Studies in Systems, Decision and Control, 2021, Vol. 345, pp. 1-15. ISBN 978-3-030-67055-9.

[COMSOL 2023] Information on [www.comsol.com/models](http://www.comsol.com/models).

[COMSOL Multiphysics 2020] Introduction to COMSOL

Multiphysics. Information on <https://pdf4pro.com/amp/view/introduction-to-comsol-multiphysics-73d842.html>

[Evin 2001] Evin, E., Hrivnak, A., Kmec, J. Data acquisition for numerical simulation. In: Technologia 2001, STU Bratislava, Vol. 1, pp. 281-284, 2001.

[Evin 2016] Evin, E., Tomas, M., Vyrostek, M. Laser-beam welding impact on the deformation properties of stainless steels when used for automotive applications. Acta Mechanica et Automatica, 2016, Vol. 10, No. 3, pp. 189-194. ISSN 1898-4088.

[Hlavac 2018] Hlavac, L.M. et al. Deformation of products cut on AWJ x-y tables and its suppression. In: International Conference on Mechanical Engineering and Applied Composite Materials, IOP Publishing, London, IOP Conference Series-Materials Science and Engineering, 2018, Vol. 307, UNSP 012015, pp. 1-10.

[Huang 2002] Huang, M. Vehicle Crash Mechanics. Boca Raton: CRC Press, 2002.

[Johnson 1983] Johnson, G.R., Cook, W.H. A constitutive model and data for metals subjected to large strains, high strain and high temperatures. In: Proceedings of the 7th International Symposium on Ballistics. Hague, Netherlands, 19-21 April 1983, pp. 541-547.

[Krenicky 2022] Krenicky, T., Olejarova, S., Servatka, M. Assessment of the Influence of Selected Technological Parameters on the Morphology Parameters of the Cutting Surfaces of the Hardox 500 Material Cut by Abrasive Water Jet Technology. Materials, 2022, Vol. 15, 1381.

[Kuncicka 2021] Kuncicka, L., Jopek, M., Kocich, R., Dvorak, K. Determining Johnson-Cook Constitutive Equation for Low-Carbon Steel via Taylor Anvil Test. Materials, 2021, Vol. 14, 4821. <https://doi.org/10.3390/ma14174821>.

[Labellarte 2000] Labellarte, A., Rizzo, L., Sebastiani, C. High Strain Rate Forming Limit Diagram for Steel and Titanium with an Optimised Methodology. In: IDDRG Working Group 2 Materials, Ann Arbor Michigan: IDDRG, 2000.

[Lin 2010] Lin, Y.C., Chen, Xiao-Min., Liu, Ge. A modified Johnson-Cook model for tensile behaviors of typical high-strength alloy steel. Materials Science and Engineering A, 2010, Vol. 527, pp. 6980-6986.

[Mathworks R2014a] Mathworks. Available from <http://www.mathworks.com/help/toolbox>, 2014.

[Murcinkova 2013] Murcinkova, Z., Krenicky, T. Applications utilizing the damping of composite microstructures for mechanisms of production machines and manipulator devices. In: SGEM 2013: 13th Int. Multidisciplinary Sci. Geoconf. Vol. 1: 16-22 June, 2013, Albena, Bulgaria. Sofia: STEF92 Technology, 2013. pp. 23-30. ISBN 978-954-91818-90.

[Vik 2003] Vik, F. Construction of motor vehicles. 1st Ed. Brno, 2003, 499 p. ISBN 80-238-8757-2.

[Wang 2021] Wang, Y., Zeng, X., Chen, H., Yang, X., Wang, F., Zeng, L. Modified Johnson-Cook constitutive

model of metallic materials under a wide range of temperatures and strain rates. Results in Physics, 2021, Vol. 27, 104498.

**CONTACTS:**

**RNDr. Jozef Kmec, PhD.**

**Prof. PaedDr. Jozef Pavelka, PhD.**

**PaedDr. Jaroslav Soltes, PhD.**

University of Presov

Faculty of Humanities and Natural Sciences

17 Novembra 15

080 01 Presov, Slovakia

[jozef.kmec@unipo.sk](mailto:jozef.kmec@unipo.sk);

[jozef.pavelka@unipo.sk](mailto:jozef.pavelka@unipo.sk)